Journal of ELECTRICAL ENGINEERING, VOL. 64, NO. 2, 2013, 100–105

USER–PARAMETER–FREE ROBUST ADAPTIVE BEAMFORMING ALGORITHM FOR VECTOR–SENSOR ARRAYS WITHIN THE HYPERCOMPLEX FRAMEWORK

Xiaoming Gou — Zhiwen Liu — Jingyan Ma — Yougen Xu *

The major flaw of the conventional diagonal loading (DL) method is that it is unclear to choose appropriate DL levels or user-parameters (UPs), though several remarkable contributions have been made to regularize model errors without UPs. An UP-free algorithm for two-component vector-sensor arrays, which is robust to steering vector errors, is considered. The algorithm is within the hypercomplex framework using quaternions, and the optimal solution is found at the maximal correlation between the quaternionic and complex outputs. The performance of the proposed beamformer is illustrated via numerical simulations and is compared with several other UP-free adaptive beamformers.

K e y w o r d s: array signal processing, robust adaptive beamforming, vector-sensor, user-parameter-free, quaternion

1 INTRODUCTION

Under idealistic assumptions (*ie*, the precise knowledge of the covariance matrix and the steering vector), the standard Capon beamformer (SCB) [1] is statistically equivalent to the optimal beamformer which maximizes the output signal-to-interference-plus-noise ratio (SINR) [2]. However, these assumptions often fail due to reasons such as the limited data length and inaccurate knowledge of the look direction or the array manifold. These factors would lead to degeneration in the performance of SCB and the signal-of-interest (SOI) might be nulled if the factors become important [3–5].

The diagonal loading (DL) method is the most widely used technique to regularize the errors [6]. Traditional DL methods, such as the norm constrained Capon beamformer (NCCB) [6] and the loaded sample matrix inversion (LSMI) [7], determine the DL level in improvised and unclear ways. Then some steering-vector-uncertainty-set-based approaches have been proposed which can provide precise DL level computation [5, 8–11]. However, the results are related to the size of the uncertainty set which might be difficult to choose in practical scenarios [12]. Those algorithms mentioned above need user-parameters (UPs) while there are only a few UP-free approaches in the literature.

A class of UP-free algorithms named ridge regression Capon beamformers (RRCBs) [13], which are based on the generalized sidelobe canceler (GSC) parameterizations, have attracted increasing attention, though other techniques such as shrinkage and power matching are also studied. Typical UP-free methods include the Hoerl Kennard Baldwin method (HKB) [14, 15], the mid-way (MW) method [16], and general linear combination (GLC) [12]. These methods are generally designed to achieve better estimates or reduce the singularity of the covariance matrix, and are able to deal with difficult conditions when the data length is quite limited.

We try to rectify model errors in a high-dimensional algebra framework, namely quaternions [17], compared with the two-dimensional space of complex numbers. Motivated by the quaternion MUSIC (Q-MUSIC) direction-finding algorithm [18], we consider the beamforming for two-component vector-sensor arrays using quaternions. A vector-sensor comprises two or more collocated different types of scalar-sensors and is generally advantageous over a scalar-sensor, *eg*, for an electromagnetic vector-sensor, it can additionally exploit the polarization difference among the received signals [19]. Traditionally the output of a vector-sensor array is preprocessed to be a long-vector [19–27], while several recent approaches utilize hypercomplex (*eg*, quaternion [18], bicomplex [28], biquaternion [29, 30], quad-quaternion [31], Euclidean 3-space [32]) or tensorial (*eg*, fourth-order interspectral tensor [33]) models. The use of hypercomplex algebra provides a compact way of handling of the recorded data, and demonstrates its unique characteristics in reduced memory consumption and improved robustness to model errors [18].

We have proposed a standard quaternion Capon (Q-Capon) for two-component vector-sensor arrays in [34]. Even though the hypercomplex-algebra-based algorithms are proved to be less sensitive to various type of errors, the Q-Capon beamformer is far from the concept of robust adaptive beamforming. Motivated by the spectral self-coherence restoral (SCORE) algorithm which is designed for blind extraction of cyclostationary signals [35], we present a UP-free DL approach, based on the maximal correlation between the quaternion output and its complex part.

* School of Information and Electronics, Beijing Institute of Technology, Beijing 100081, People's Republic of China, xmgou@bit.edu.cn, zwliu@bit.edu.cn, majy@bit.edu.cn, yougenxu@bit.edu.cn

DOI: 10.2478/jee-2013-0014, ISSN 1335-3632

The rest of the paper is organized as follows. In Section 2, we introduce the quaternion algebra and the Q-Capon beamformer. Then we formulate the proposed robust approach in Section 3 and provide some numerical examples compared with several UP-free algorithms in Section 4. Finally, we give the conclusion in Section 5.

2 QUATERNION CAPON BEAMFORMER

2.1 Quaternions

Hamilton's quaternions form a four-dimensional (4D) space. In this paper, we denote the sets of real numbers, complex numbers with imaginary unit of $\mathfrak{i}$, and quaternions, as $\mathbb{R}$, $\mathbb{C}$, and $\mathbb{H}$, respectively. A quaternion $q \in \mathbb{H}$ comprises one real and three imaginary parts, namely

$$q = q^r + \mathfrak{i}q^i + \mathfrak{j}q^j + \mathfrak{k}q^k \tag{1}$$

where $q^r, q^i, q^j, q^k \in \mathbb{R}$ and the imaginary units $\mathfrak{i}$, $\mathfrak{j}$, and $\mathfrak{k}$ are subject to the following constraints

$$\begin{aligned} &\mathfrak{i}^2 = \mathfrak{j}^2 = \mathfrak{k}^2 = -1\,, \\ &\mathfrak{ij} = -\mathfrak{ji} = \mathfrak{k}, \mathfrak{jk} = -\mathfrak{kj} = \mathfrak{i}, \mathfrak{ki} = -\mathfrak{ik} = \mathfrak{j}\,. \end{aligned} \tag{2}$$

Various details about quaternions can be found in articles and books like [18], [36], [37], and part of them that will be used in this paper are shown below:

(1) The Cayley-Dickson form of q is given by $q = q^c + \mathfrak{j}q^e$, where $q^c = q^r + \mathfrak{i}q^i$ and $q^e = q^j - \mathfrak{i}q^k$.

(2) The quaternion algebra is not multiplicatively commutative, *ie*, generally, for two quaternions $a, b \in \mathbb{H}$, $ab \neq ba$.

(3) The conjugate of q, denoted by $q^\diamond$, is defined as $q^\diamond = q^r - \mathfrak{i}q^i - \mathfrak{j}q^j - \mathfrak{k}q^k$. If $q^\diamond = q$, then $q^r = 0$, and q is a pure quaternion. For two quaternions $a, b \in \mathbb{H}$, there holds $(ab)^\diamond = b^\diamond a^\diamond$. The conjugate transpose of a quaternion matrix $\mathbf{Q} \in \mathbb{H}^{N\times M}$, denoted by $\mathbf{Q}^\dagger$, is defined as $\mathbf{Q}^\dagger = \mathbf{Q}^{r\mathrm{T}} - \mathfrak{i}\mathbf{Q}^{i\mathrm{T}} - \mathfrak{j}\mathbf{Q}^{j\mathrm{T}} - \mathfrak{k}\mathbf{Q}^{k\mathrm{T}}$, where superscript $^\mathrm{T}$ signifies transpose. For two quaternion matrices $\mathbf{A} \in \mathbb{H}^{N\times M}, \mathbf{B} \in \mathbb{H}^{M\times K}$, there holds $(\mathbf{AB})^\dagger = \mathbf{B}^\dagger\mathbf{A}^\dagger$.

(4) The modulus of a quaternion $q \in \mathbb{H}$ and the norm of a quaternion vector $\boldsymbol{q} \in \mathbb{H}^{N\times 1}$ are respectively given by $|q| = \sqrt{q^\diamond q}$ and $||\boldsymbol{q}|| = \sqrt{\boldsymbol{q}^\dagger \boldsymbol{q}}$.

(5) A quaternion matrix $\mathbf{Q}$ is Hermitian if $\mathbf{Q}^\dagger = \mathbf{Q}$. The eigenvalue decomposition of a Hermitian quaternion matrix $\mathbf{Q} \in \mathbb{H}^{N\times N}$ is given by $\mathbf{Q} = \mathbf{U}\boldsymbol{\Lambda}\mathbf{U}^\dagger$, where $\boldsymbol{\Lambda} \in \mathbb{R}^{N\times N}$ is a diagonal matrix containing the eigenvalues and $\mathbf{U} \in \mathbb{H}^{N\times N}$ is comprised of the eigenvectors.

(6) A quaternion matrix $\mathbf{Q}$ is invertible if there exists a matrix over $\mathbb{H}$, denoted by $\mathbf{Q}^{-1}$, such that $\mathbf{Q}\mathbf{Q}^{-1} = \mathbf{Q}^{-1}\mathbf{Q} = \mathbf{I}$, where $\mathbf{I}$ signifies an identity matrix.

2.2 Quaternion Capon beamformer

We assume an array composed of N two-component vector-sensors. One far-field narrowband SOI $s_0(t) \in \mathbb{C}$ impinges on the array in the presence of M co-channel independent interferences $\{s_m(t)\}_{m=1}^M \in \mathbb{C}$ and background white Gaussian noise $\boldsymbol{n}_1(t), \boldsymbol{n}_2(t) \in \mathbb{C}^{N\times 1}$. The two measurement vectors $\mathbf{x}_1(t), \mathbf{x}_2(t) \in \mathbb{C}^{N\times 1}$ of the two subarrays are respectively given by

$$\begin{aligned} \mathbf{x}_1(t) &= \sum_{m=0}^{M} \boldsymbol{a}_{m,1} s_m(t) + \boldsymbol{n}_1(t)\,, \\ \mathbf{x}_2(t) &= \sum_{m=0}^{M} \boldsymbol{a}_{m,2} s_m(t) + \boldsymbol{n}_2(t)\,. \end{aligned} \tag{3}$$

A quaternion-valued output vector $\boldsymbol{q}(t) \in \mathbb{H}^{N\times 1}$ is constructed as

$$\boldsymbol{q}(t) = \mathbf{x}_1(t) + \mathfrak{j}\mathbf{x}_2(t) = \sum_{m=0}^{M} \boldsymbol{a}_m s_m(t) + \boldsymbol{n}(t) \tag{4}$$

$$\begin{aligned} &\boldsymbol{a}_m = \boldsymbol{a}_{m,1} + \mathfrak{j}\boldsymbol{a}_{m,2} \in \mathbb{H}^{N\times 1}, \quad m = 0, 1, \dots, M\,, \\ &\boldsymbol{n}(t) = \boldsymbol{n}_1(t) + \mathfrak{j}\boldsymbol{n}_2(t) \in \mathbb{H}^{N\times 1}\,. \end{aligned} \tag{5}$$

Then the quaternion Capon weight vector $\boldsymbol{w} \in \mathbb{H}^{N\times 1}$ is given by (see [34] for details)

$$\boldsymbol{w} = \frac{\mathbf{R}^{-1}\mathbf{a}_0}{\mathbf{a}_0^\dagger \mathbf{R}^{-1}\mathbf{a}_0} \tag{6}$$

$$\mathbf{R} = E\{\boldsymbol{q}(t)\boldsymbol{q}^\dagger(t)\} \in \mathbb{H}^{N\times N} \tag{7}$$

is the Hermitian covariance matrix and the quaternion-valued output $y(t) \in \mathbb{H}$ of the beamformer is given by

$$y(t) = \mathbf{w}^\dagger \mathbf{a}_0 s_0(t) + \sum_{m=1}^{M} \mathbf{w}^\dagger \mathbf{a}_M s_M(t) + \mathbf{w}^\dagger \boldsymbol{n}(t) \tag{8}$$

where $\mathbf{w}^\dagger \mathbf{a}_0 = 1$ and $\mathbf{w}^\dagger \mathbf{a}_m \approx 0, m = 1, \dots, M$ which indicates that the interferences are nulled and the SOI is extracted [34]. In idealistic scenarios, $s_0(t)$ only exists in $y^c(t) \in \mathbb{C}$ from (8). In the presence of model errors, $s_0(t)$ exists in both $y^c(t)$ and $y^e(t)$, while their mutual phase delay is hard to be accurately estimated. Hence we use $y^c(t)$ as the output.

3 USER–PARAMETER–FREE ROBUST QUATERNION CAPON BEAMFORMER

In practical scenarios, the presumed steering vector $\bar{\mathbf{a}}_0$ can deviate from the actual one due to reasons like look direction error and poor covariance matrix estimation (which can be also equivalently viewed as a type of steering error), leading to undesired conditions such as self-nulling (*ie*, the SOI is nulled) and sequentially great

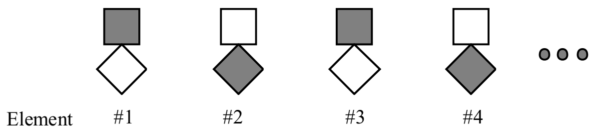

Fig. 1. The subarray configuration: stacked square and diamond – vector-sensor with collocated components, square – type-A sensor, filled – subarray #1, diamond – type-B sensor, unfilled – subarray #2

degeneration in the beamforming performance. We consider the diagonal loading technique to compensate the steering error (where μ denotes the loading level),

$$\begin{aligned}\tilde{\mathbf{R}} &= \tilde{\mathbf{R}}(\mu) = \mathbf{R} + \mu\mathbf{I}\,,\\ \boldsymbol{w} &= \boldsymbol{w}(\mu) = \frac{\tilde{\mathbf{R}}^{-1}(\mu)\bar{\mathbf{a}}_0}{\bar{\mathbf{a}}_0^\dagger\tilde{\mathbf{R}}^{-1}(\mu)\bar{\mathbf{a}}_0}\,.\end{aligned} \tag{9}$$

In the presence of considerable steering vector errors, we consider the following progress:

(1) For a relatively small μ, the beamformer is directed to noise due to the steering vector errors and all the signals are nulled, and $y(t)$ is almost a mixture of element noise, *ie*,

$$\begin{aligned}y(t,\mu) &\approx \boldsymbol{w}^\dagger(\mu)\boldsymbol{n}(t)\,,\\ z(t,\mu) &= y^c(t,\mu) \approx [\boldsymbol{w}^\dagger(\mu)\boldsymbol{n}(t)]^c\,.\end{aligned} \tag{10}$$

Then the cross-correlation coefficient between $y(t,\mu)$ and $z(t,\mu)$ is given by (the derivation can be found in Appendix A)

$$\rho_{yz}(\mu) = \frac{\left|E_t\{y(t,\mu)z^\diamond(t,\mu)\}\right|}{\sqrt{E_t\{|y(t,\mu)|^2\}}\sqrt{E_t\{|z(t,\mu)|^2\}}} \approx \frac{1}{\sqrt{2}}\,. \tag{11}$$

(2) As μ increases, the self-nulling problem is alleviated. When μ rises to a very good value, the beamformer is approximately redirected to the actual direction and the SOI is perfectly extracted, namely

$$\begin{aligned}\boldsymbol{w}(\mu) &\approx \mathbf{R}^{-1}\mathbf{a}_0\tau\,,\\ y(t,\mu) &\approx \tau^\diamond\mathbf{a}_0^\dagger\mathbf{R}^{-1}\mathbf{a}_0 s_0(t) = \iota s_0(t)\,,\\ z(t,\mu) &= y^c(t,\mu) \approx \iota^c s_0(t)\,,\end{aligned} \tag{12}$$

where $\tau, \iota \in \mathbb{H}$. Then $\rho_{yz}(\mu)$ is given by

$$\rho_{yz}(\mu) = \frac{\left|E_t\{y(t,\mu)z^\diamond(t,\mu)\}\right|}{\sqrt{E_t\{|y(t,\mu)|^2\}}\sqrt{E_t\{|z(t,\mu)|^2\}}} \approx 1\,. \tag{13}$$

(3) As μ goes on to increase, the leakage problems (*ie*, the interferences remain in the output of the beamformer) emerge and deteriorate, which drags the ρ_{yz} down.

Hence we can form an optimization problem to find a desired μ which is given by

$$\hat{\mu} = \arg\max_{\mu} \rho_{yz}(\mu)\,. \tag{14}$$

It should be noted that when μ approaches infinity, the beamformer is approximately equal to the classic delay-and-sum beamformer (DAS, also named Bartlett beamformer), namely $\boldsymbol{w} \approx \bar{\mathbf{a}}_0$, in which case the most serious leakage problem happens. The gain of the DAS at the m-th signal is the projection of the vector $\boldsymbol{a}_m$ onto the vector $\bar{\mathbf{a}}_0$. If the two subarrays are categorized conventionally by the types of the sensors (*eg*, for a crossed-dipole array, sensors measuring E_x and E_y incident electric fields belong to subarray #1 and subarray #2, respectively), their steering vectors of the same signal are colinear, namely $\boldsymbol{a}_{m,1}//\boldsymbol{a}_{m,2}$, which leads to $\boldsymbol{a}_m//\boldsymbol{a}_{m,1}//\boldsymbol{a}_{m,2}$. Hence $y(t,\mu)$ and $z(t,\mu)$ can be highly correlated, which indicates a large ρ_{yz}. To avoid this undesired situation, we divide the array into two arrays in a ping-pong manner, which can guarantee the non-colinearity without ambiguity since no inter-element spacings have changed, as is shown in Fig. 1.

It is easily verified that $z(t,\mu)$ can be rewritten as

$$z(t,\mu) = y^c(t,\mu) = \frac{y(t,\mu) - \mathfrak{i}y(t,\mu)\mathfrak{i}}{2}\,. \tag{15}$$

Thus we can reformulate (14) as

$$\hat{\mu} = \arg\max_{\mu} \rho_{yd}(\mu), \quad d(t,\mu) = \mathfrak{i}y(t,\mu)\mathfrak{i} \tag{16}$$

Since

$$\begin{aligned}E_t\big\{|d(t,\mu)|^2\big\} = E_t\big\{|y(t,\mu)|^2\big\} &= \boldsymbol{w}^\dagger(\mu)\mathbf{R}\boldsymbol{w}(\mu)\,,\\ E_t\big\{y(t,\mu)d^\diamond(t,\mu)\big\} &= \boldsymbol{w}^\dagger(\mu)\mathbf{C}\boldsymbol{w}(\mu)\mathfrak{i}\end{aligned} \tag{17}$$

where

$$\mathbf{C} = E\{\boldsymbol{q}(t)\mathfrak{i}\boldsymbol{q}^\dagger(t)\} \in \mathbb{H}^{N\times N}, \mathbf{C}^\dagger = -\mathbf{C}\,. \tag{18}$$

Then $\rho_{yd}(\mu)$ is given by

$$\begin{aligned}\rho_{yd}(\mu) &= \frac{\left|E_t\big\{y(t,\mu)d^\diamond(t,\mu)\big\}\right|}{\sqrt{E_t\big\{|y(t,\mu)|^2\big\}}\cdot\sqrt{E_t\big\{|d(t,\mu)|^2\big\}}}\\ &= \frac{\left|\boldsymbol{w}^\dagger(\mu)\mathbf{C}\boldsymbol{w}(\mu)\right|}{\boldsymbol{w}^\dagger(\mu)\mathbf{R}\boldsymbol{w}(\mu)}\,.\end{aligned} \tag{19}$$

Since there are no clear guidelines to choose the upper limit of μ, here we use an alternate formulation called convex combination (CC) [38, 39], namely,

$$\begin{aligned}\tilde{\mathbf{R}} &= \tilde{\mathbf{R}}(\alpha) = (1-\alpha)\mathbf{R} + \alpha\mathbf{I}\,, \quad 0 \le \alpha \le 1\,,\\ \boldsymbol{w} &= \boldsymbol{w}(\alpha) = \frac{\tilde{\mathbf{R}}^{-1}(\alpha)\bar{\mathbf{a}}_0}{\bar{\mathbf{a}}_0^\dagger\tilde{\mathbf{R}}^{-1}(\alpha)\bar{\mathbf{a}}_0}\end{aligned} \tag{20}$$

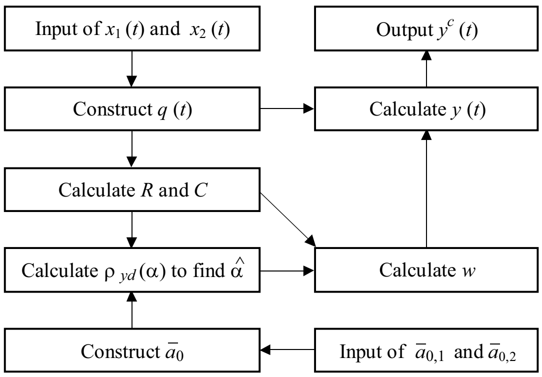

Fig. 2. Flowchart of RQ-Capon beamformer

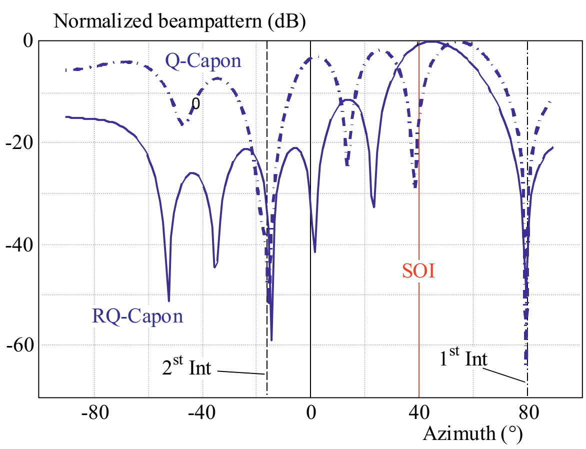

Fig. 3. Normalized beampatterns

which compresses the infinite interval $\mu \in [0, \infty)$ into the finite interval $\alpha \in [0, 1]$ nonlinearly. Then we can rewrite (16) as

$$\hat{\alpha} = \arg \max_{0 \le \alpha \le 1} \rho_{yd}(\alpha) \tag{21}$$

where

$$\begin{aligned} \rho_{yd}(\alpha) &= \frac{\left| \boldsymbol{w}^\dagger(\alpha) \mathbf{C} \boldsymbol{w}(\alpha) \right|}{\boldsymbol{w}^\dagger(\alpha) \mathbf{R} \boldsymbol{w}(\alpha)} \\ &= \frac{\left| \bar{\mathbf{a}}_0^\dagger [(1-\alpha)\mathbf{R} + \alpha \mathbf{I})]^{-1} \mathbf{C} [(1-\alpha)\mathbf{R} + \alpha \mathbf{I}]^{-1} \bar{\mathbf{a}}_0 \right|}{\bar{\mathbf{a}}_0^\dagger [(1-\alpha)\mathbf{R} + \alpha \mathbf{I})]^{-1} \mathbf{R} [(1-\alpha)\mathbf{R} + \alpha \mathbf{I})]^{-1} \bar{\mathbf{a}}_0} . \end{aligned} \tag{22}$$

We name the beamformer formulated above as robust quaternion Capon beamformer (RQ-Capon), which is an user-parameter-free algorithm. The flowchart of the RQ-Capon beamformer is illustrated in Fig. 2, and the two performance evaluation criterions, namely SINR (signal-to-interference-plus-noise ratio) and SOI power estimate are respectively given by

$$\mathrm{SINR} = \frac{\sigma_0^2 |(\boldsymbol{w}^\dagger \boldsymbol{a}_0)^c|^2}{\sigma_{\mathrm{n}}^2 ||\boldsymbol{w}||^2 + \sum_{m=1}^{M} \sigma_m^2 |(\boldsymbol{w}^\dagger \boldsymbol{a}_m)^c|^2} , \tag{23}$$

$$\begin{aligned} \hat{\sigma}_0^2 &= E\{|[\boldsymbol{w}^\dagger \boldsymbol{q}(t)]^c|^2\} = \\ &(\boldsymbol{w}^c)^\dagger \mathbf{R}_{11} \boldsymbol{w}^c + 2[(\boldsymbol{w}^c)^\dagger \mathbf{R}_{12} \boldsymbol{w}^e]^r + (\boldsymbol{w}^e)^\dagger \mathbf{R}_{22} \boldsymbol{w}^e \end{aligned} \tag{24}$$

where σ_{n}^2 denotes the noise power (see remaining power computation in (27)) and

$$\begin{aligned} \mathbf{R}_{11} &= E\{\mathbf{x}_1(t)\mathbf{x}_1^\dagger(t)\} , \\ \mathbf{R}_{22} &= E\{\mathbf{x}_2(t)\mathbf{x}_2^\dagger(t)\} , \\ \mathbf{R}_{12} &= E\{\mathbf{x}_1(t)\mathbf{x}_2^\dagger(t)\} , \\ \boldsymbol{w} &= \frac{[(1-\hat{\alpha})\mathbf{R} + \hat{\alpha}\mathbf{I}]^{-1} \bar{\mathbf{a}}_0}{\bar{\mathbf{a}}_0^\dagger [(1-\hat{\alpha})\mathbf{R} + \hat{\alpha}\mathbf{I}]^{-1} \bar{\mathbf{a}}_0} . \end{aligned} \tag{25}$$

4 SIMULATIONS

In this section, we provide some numerical examples to illustrate the performance of the proposed beamformer comparing it with several UP-free robust beamformers, i.e., GLC, HKB, and MW. The non-robust version of RQ-Capon, namely Q-Capon is also shown for comparison. In all the examples, we assume a uniform linear array (ULA) composed of 8 crossed-dipole antennas (measuring E_x and E_y incident electric fields) spaced half wavelength apart. The incident signals are assumed to be far-field narrowband, and the noises of 0 dB power are complex-valued zero-mean additive white Gaussian. One SOI of 15 dB power from 40° (azimuth) and two interfering signals both of 30 dB power from 80° and −15° (azimuth) impinge on the array, respectively.

In the first example, we set the number of snapshots to 200. For the convenience of beampattern visualization, we assume the three signals shares the same elevation and polarization angles as 45° and $(45°, 0°)$, respectively. Fig. 3 shows the normalized beampattern (acquired by plotting $10\log_{10}\{|[\mathbf{w}^\dagger \mathbf{a}(\theta)]^c|^2\}$) of RQ-Capon and Q-Capon when the presumed SOI angle is 44° (i.e., a 4° error), where the three vertical lines indicate the angles of three sources. It can be seen that RQ-Capon has a robust response at the SOI when look direction error exists, while Q-Capon suffers a self-nulling problem.

The results below are all averaged via 1000 Monte-Carlo simulation runs.

In the second example, we test robustness of the beamformers in terms of output SINR and SOI power estimation. The elevation angles of the SOI and two interferences are $25°, 65°, 45°$, respectively, while their polarization angles are $(45°, 0°), (10°, 85°), (75°, 30°)$, respectively. The presumed SOI angles are $(42°, 27°, 43°, 2°)$, which means a 3° error in every parameter. Fig. 4 and Fig. 5 illustrate the output SINR and SOI power estimates versus number of snapshots, respectively. The optimal (or maximally achievable) SINR and the real SOI power are also shown for comparison. It can be seen that higher SINR values and more accurate SOI power estimates are achieved by RQ-Capon. The improvements are

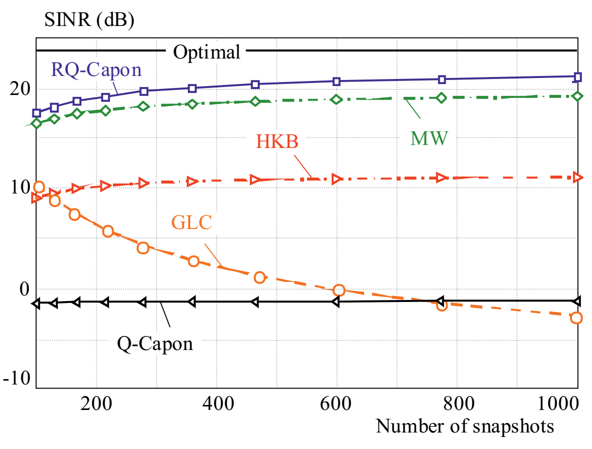

Fig. 4. SINR versus number of snapshots

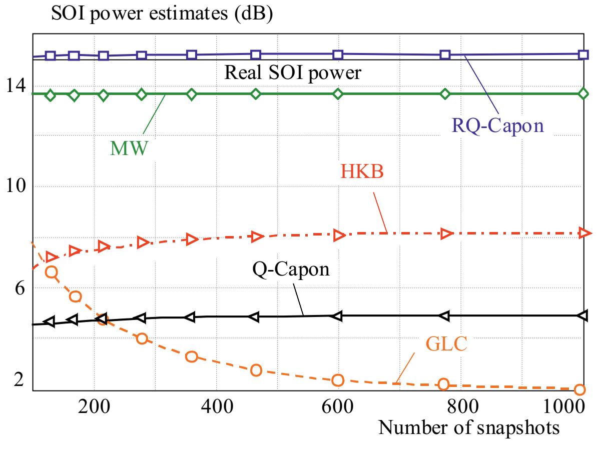

Fig. 5. Power estimates versus number of snapshots

mainly due to RQ-Capon's additional exploitation of the subarray feature within the hypercomplex modelling.

5 CONCLUSIONS

We have proposed a cross-SCORE-based robust adaptive beamformer (named RQ-Capon) in the hypercomplex framework for sensor arrays of two-component vector sensors, which selects the diagonal loading levels via a finite-interval searching scheme without specifying any user-parameter. We have demonstrated via numerical examples that RQ-Capon is superior compared with several other user-parameter-free approaches in terms of both SINR and SOI power estimation. To conclude the paper, we note that RQ-Capon can also be performed on any scalar-sensor array with two equal-dimensional non-overlapping rotational-variant subarrays.

APPENDIX: A Computation in (11)

For simplicity, μ is omitted, then

$$E\{|y(t)|^2\} \approx \mathbf{w}^\dagger E\{[\boldsymbol{n}_1(t) + \jmath\boldsymbol{n}_2(t)][\boldsymbol{n}_1^\dagger(t) - \boldsymbol{n}_2^\dagger(t)\jmath]\}\boldsymbol{w} = 2\sigma_{\rm n}^2\|\mathbf{w}\|^2, \quad (26)$$

$$E\{|z(t)|^2\} \approx E\{|(\mathbf{w}^c)^\dagger \boldsymbol{n}_1(t) + (\mathbf{w}^e)^\dagger \boldsymbol{n}_2(t)|^2\} = \sigma_{\rm n}^2(||\mathbf{w}^c||^2 + ||\mathbf{w}^e||^2) = \sigma_{\rm n}^2||\mathbf{w}||^2, \quad (27)$$

$$|E\{y(t)z^\diamond(t)\}| \approx |\mathbf{w}^\dagger[\boldsymbol{n}_1(t) + \jmath\boldsymbol{n}_2(t)][\boldsymbol{n}_1^\dagger(t)\mathbf{w}^c + \boldsymbol{n}_2^\dagger(t)\mathbf{w}^e]| = \sigma_{\rm n}^2|\mathbf{w}^\dagger\mathbf{w}^c + \mathbf{w}^\dagger\jmath\mathbf{w}^e| = \sigma_{\rm n}^2||\mathbf{w}||^2. \quad (28)$$

Hence

$$\rho_{yz} \approx \frac{\sigma_{\rm n}^2||\mathbf{w}||^2}{\sqrt{2\sigma_{\rm n}^2||\mathbf{w}||^2}\cdot\sqrt{\sigma_{\rm n}^2||\mathbf{w}||^2}} = \frac{1}{\sqrt{2}}. \quad (29)$$

Acknowledgements

This work was supported by National Natural Science Foundation of China (No. 61072098, 61072099).

References

[1] CAPON, J.: High-Resolution Frequency-Number Spectrum Analysis, Proceedings of the IEEE **57** No. 8 (Aug 1969), 1408–1418.

[2] APPLEBAUM, S. P.: Adaptive Arrays, IEEE Transactions on Antennas Propagation **AP-24** No. 5 (Sep 1976), 585–1976.

[3] COX, H.: Resolving Power and Sensitivity to Mismatch of Optimum Array Processors, Journal of the Acoustical Society of America **54** No. 3 (Sep 1973), 771–785.

[4] FELDMAN, D. D.—GRIFFITHS, L. J.: A Projection Approach for Robust Adaptive Beamforming, IEEE Transactions on Signal Processing **42** No. 4 (April 1994), 867–876.

[5] LI, J.—STOICA, P.: Robust Adaptive Beamforming, Wiley, New York, 2005.

[6] COX, H.—ZESKIND, R. M.—OWEN, M. M.: Robust Adaptive Beamforming, IEEE Transactions on Acoustics, Speech, and Signal Processing **ASSP-35** No. 10 (Oct 1987), 1365–1375.

[7] CARLSON, B. D.: Covariance-Matrix Estimation Errors and Diagonal Loading in Adaptive Arrays, IEEE Transactions on Aerospace and Electronic Systems **24** No. 4 (July 1970), 397-401.

[8] VOROBYOV, S. A.—GERSHMAN, A. B.—LUO, Z. Q.: Robust Adaptive Beamforming using Worst-Case Performance Optimization: A Solution to the Signal Mismatch Problem, IEEE Transactions on Signal Processing **51** No. 2 (Feb 2003), 313–324.

[9] LI, J.—STOICA, P.—WANG, Z. S.: On Robust Capon Beamforming and Diagonal Loading, IEEE Transactions on Signal Processing **51** No. 7 (July 2003), 1702–1715.

[10] LI, J.—STOICA, P.—WANG, Z. S.: Doubly Constrained Robust Capon Beamformer, IEEE Transactions on Signal Processing **52** No. 9 (Sep 2004), 2407–2423.

[11] LORENZ, R. G.—BOYD, S. P.: Robust Minimum Variance Beamforming, IEEE Transactions on Signal Processing **53** No. 5 (May 2005), 1684–1696.

[12] DU, L.—LI, J.—STOICA, P.: Fully Automatic Computation of Diagonal Loading Levels for Robust Adaptive Beamforming, IEEE Transactions on Aerospace and Electronic Systems **46** No. 1 (Jan 2010), 449–458.

[13] VERDÚ, S.—POOR, H. V.: Minimax Robust Discrete-Time Matched Filters, IEEE Transactions on Communications **CO M-31** No. 2 (Feb 1983), 208–215.

[14] HOERL, A. E.—KANNARD, R. W.—BALDWIN, K. F.: Ridge Regression: Some Simulations, Communication in Statistics: Theory and Methods **4** No. 2 (1975), 105–123.

[15] SELÉN, Y.—ABRAHAMSSON, R.—STOICA, P. : Automatic Robust Adaptive Beamforming via Ridge Regression, Signal Processing **88** No. 1 (Jan 2008), 33–49.

[16] STOICA, P.—LI, J.—TAN, X. : On Spatial Power Spectrum and Signal Estimation using the Pisarenko Framework, IEEE Transactions on Signal Processing **56** No. 10 (Oct 2008), 5109–5119.

[17] HAMILTON, W. R. : On Quaternions, Proceedings of the Royal Irish Academy **3** (1847), 1–16.

[18] MIRON, S.—LE BIHAN, N.—MARS, J. I. : Quaternion MUSIC for Vector-Sensor Array Processing, IEEE Transactions Signal Processing **54** No. 4 (Apr 2006), 1218–1229.

[19] NEHORAI, A.—PALDI, E. : Vector-Sensor Array Processing for Electromagnetic Source Localization, IEEE Transactions on Signal Processing **42** No. 2 (Feb 1994), 376–398.

[20] NEHORAI, A.—PALDE, E. : Acoustic Vector-Sensor Array Processing, IEEE Transactions on Signal Processing **42** No. 9 (Sep 1994), 2481–2491.

[21] WONG, K. T.—ZOLTOWSKI, M. D. : Root-MUSIC-Based Azimuth-Elevation Angle-of-Arrival Estimation with Uniformly Spaced but Arbitrarily Oriented Velocity Hydrophones, IEEE Transactions on Signal Processing **47** No. 12 (Dec 1999), 3250–3260.

[22] WONG, K. T.—ZOLTOWSKI, M. D. : Self-Initiating MUSIC-Based Direction Finding and Polarization Estimation in Spatio-Polarizational Beamspace, IEEE Transactions on Antennas and Propagation **48** No. 8 (Aug 2000), 1235–1245.

[23] WONG, K. T.—ZOLTOWSKI, M. D. : Closed-Form Direction Finding and Polarization Estimation with Arbitrarily Spaced Electromagnetic Vectorsensors at Unknown Locations, IEEE Transactions on Antennas and Propagation **48** No. 5 (May 2000), 671–681.

[24] ZOLTOWSKI, M. D.—WONG, K. T. : ESPRIT-Based 2-D Direction Finding with a Sparse Uniform Array of Electromagnetic Vector Sensors, IEEE Transactions on Signal Processing **48** No. 8 (Aug 2000), 2195–2204.

[25] ZOLTOWSKI, M. D.—WONG, K. T. : Closed-Form Eigenstructure-Based Direction Finding using Arbitrary but Identical Subarrays on a Sparse Uniform Cartesian Array Grid, IEEE Transactions on Signal Processing **48** No. 8 (Aug 2000), 2205–2210.

[26] LI, J.—COMPTON, R. T., jr. : Angle Estimation using a Polarization Sensitive Array, IEEE Transactions on Antennas and Propagation **39** No. 10 (Oct 1991), 1539–1543.

[27] LI, J.—COMPTON, R. T., jr. : Angle and Polarization Estimation in a Coherent Signal Environment, IEEE Transactions on Aerospace and Electronic Systems **29** No. 3 (July 1993), 706–716.

[28] GONG, X. F.—LIU, Z. W.—XU, Y. G. : Coherent Source Localization: Bicomplex Polarimetric Smoothing with Electromagnetic Vector-Sensors, IEEE Transactions on Aerospace and Electronic Systems **47** No. 3 (July 2011), 2268–2285.

[29] Le BIHAN, N.—MIRON, S.—MARS, J. I. : MUSIC Algorithm for Vector-sensors Array Processing using Biquaternions, IEEE Transactions on Signal Processing **55** No. 9 (Sep 2007), 4523–4533.

[30] GONG, X. F.—LIU, Z. W.—XU, Y. G. : Direction Finding via Biquaternion Matrix Diagonalization with Vector-Sensors, Signal Processing **91** No. 4 (Apr 2011), 821–831.

[31] GONG, X. F.—LIU, Z. W.—XU, Y. G. : Quad-Quaternion MUSIC for DOA Estimation using Electromagnetic Vector Sensors, EURASIP Journal on Advances in Signal Processing (2008), 14 pages.

[32] JIANG, J. F.—ZHANG, J. Q. : Geometric Algebra of Euclidean 3-Space for Electromagnetic Vector-Sensor Array Processing, Part I: Modeling, IEEE Transactions on Antennas and Propagation **58** No. 12 (Dec 2010), 3961–3973.

[33] MIRON, S.—Le BIHAN, N.—MARS, J. I. : Vector-Sensor MUSIC for Polarized Seismic Sources Localization, EURASIP Journal on Applied Signal Processing **2005** No. 1 (Jan 2005), 74–84.

[34] GOU, X. M.—XU, Y. G.—LIU, Z. W.—GONG, X. F. : Quaternion-Capon Beamformer using Crossed-Dipole Arrays, in Proceedings of International Symposium on Microwave, Antenna, Propagation and EMC Technologies for Wireless Communications, MAPE 2011, Beijing, China, 1–3 November 2011, 34–37.

[35] AGEE, B. G.—SCHELL, S. V.—GARDNER, W. A. : Spectral Self-Coherence Restoral: A New Approach to Blind Adaptive Signal Extraction using Antenna Arrays, Proceedings of the IEEE **78** No. 4 (Apr 1990), 753–767.

[36] TOOK, C. C.—MANDIC, D. P. : The Quaternion LMS Algorithm for Adaptive Filtering of Hypercomplex Processes, IEEE Transactions on Signal Processing **57** No. 4 (Apr 2009), 1316–1327.

[37] WARD, J. P. : Quaternions and Cayley Numbers: Algebra and Applications, Kluwer, Normwell, MA, 1997.

[38] LEDOIT, O.—WOLF, M. : A Well-Conditioned Estimator for Large-Dimensional Covariance Matrices, Journal of Multivariate Analysis **88** No. 2 (Feb 2004), 365–411.

[39] DU, L.—YARDIBI, T.—LI, J.—STOICA, P. : Review of User Parameter-Free Robust Adaptive Beamforming Algorithms, Digital Signal Processing **19** No. 4 (July 2009), 567–582.

Received 15 September 2012

Xiaoming Gouwas born in Binzhou, China, in 1988. He received the BSc degree from Beijing Institute of Technology, China, in 2010, where he is currently pursuing the PhD degree. His main research interest is array signal processing within the hypercomplex framework.

Zhiwen Liu was born in Xi'an, China, in 1962. He received the BSc degree from Xidian University, China, in 1983, and the MSc and PhD degrees from Beijing Institute of Technology, China, in 1986 and 1989, respectively. He is currently a full professor at the School of Information and Electronics, Beijing Institute of Technology. His research interests include array signal processing, video image processing, radar imaging, and detection theory. He has authored and coauthored in over 180 papers in the above areas. He is a Senior Member of the Chinese Institute of Electronics (CIE) and a co-editor of the 1996 CIE International Conference of Radar Proceedings. He received the Distinguished Younger Teacher Award and the Higher Education Teaching Award from Beijing Municipal Government in 1995 and 2001, respectively.

Jingyan Ma was born in Anyang, China, in 1986. She received the BSc degree from Northeast Normal University, China, in 2007, and the MSc degree from Beijing Institute of Technology, China, in 2009, where she is currently pursuing the PhD degree. Her main research interest is robust adaptive beamforming of communication signals.

Yougen Xu was born in Yancheng, China, in 1975. He received the BSc, MSc, and PhD degrees from Beijing Institute of Technology, China, in 1998, 2001, and 2004, respectively. He is currently an associate professor at the School of Information and Electronics, Beijing Institute of Technology. He has authored and coauthored in over 70 scientific papers. His research interests include array signal processing using regularization methods, high-order/mixed-order statistics and vector-sensors.